Revista Facultad de Ingeniería, Universidad de Antioquia, No.98, pp. 83-93, Jan-Mar 2021

A kinetic study of the photoinduced oxo-transfer using a Mo complex anchored to TiO_2

Un estudio cinético de la oxo-transferencia fotoinducida usando un complejo de Mo anclado a TiO_2

Julián E. Sánchez-Velandia [1,2*], **Edgar A. Páez-Mozo** [1], **Fernando Martínez-Ortega** [1]

[1]Centro de Investigación en Catálisis, Escuela de Química, Facultad de Ciencias, Universidad Industrial de Santander. Km 2 vía El refugio. C. P. 681011. Piedecuesta, Colombia.
[2]Grupo de Investigación Catálisis Ambiental, Departamento de Ingeniería Química, Facultad de Ingeniería, Universidad de Antioquia. Calle 70 #52-21. C. P. 050010. Medellín, Colombia.

CITE THIS ARTICLE AS:

J. E. Sánchez, E. A. Páez and F. Martínez. "A kinetic study of the photoinduced oxo-transfer using a Mo complex anchored to TiO_2", *Revista Facultad de Ingeniería Universidad de Antioquia*, no. 98, pp. 83-93, Jan-Mar 2021. [Online]. Available: https://www.doi.org/10.17533/udea.redin.20200477

ARTICLE INFO:

Received: February 01, 2020
Accepted: May 14, 2020
Available online: May 14, 2020

KEYWORDS:

Photonic flux; selective photooxidation; dioxomolybdenum complex; quantum yield

Flujo fotónico; fotooxidación selectiva; complejo dioxo-Molibdeno; rendimiento cuántico

ABSTRACT: Kinetic study of the photo-assisted oxygen atom transfer reaction (OAT) using a dioxo-Mo complex anchored on TiO_2, stimulated by light, was performed at ambient conditions using triphenylphosphine (PPh_3) as a model molecule. The kinetic of the OAT reaction was studied with three catalytic systems: 4,4'-dicarboxylate-2,2'-bipyridine-dioxochloromolybdenum (MoO_2L/TiO_2), H_2MoO_4 (H_2MoO_4/TiO_2) and molybdenum oxide (MoO_3/ TiO_2) anchored to TiO_2. The MoO_2L/TiO_2 gives conversion higher than 90% and selectivity (to phosphine oxide) close to 100%. MoO_3/TiO_2 did not allow the oxo-transference, suggesting the importance of the bipyridine ligand as an electronic connector between MoO_2L unit and TiO_2. With the MoO_2L/TiO_2 system was observed that when the photonic flux increases, the quantum yield, and the OAT reaction rate increases.

RESUMEN: El estudio cinético de la reacción de transferencia de átomos de oxígeno (TAO) foto asistida se estudió usando un complejo de dioxo-Mo anclado al TiO_2, estimulada por la luz en condiciones ambientales usando trifenilfosfina como molécula modelo. La cinética de la reacción TAO fue estudiada con tres sistemas catalíticos anclados al TiO_2: 4,4'-dicarboxilato-2,2'-bipiridina-dioxocloromolibdeno (MoO_2L/TiO_2), H_2MoO_4 (H_2MoO_4/TiO_2) y óxido de molibdeno (MoO_3/ TiO_2). El catalizador MoO_2L/TiO_2 permitió la conversión más alta del 90% y una selectividad (al óxido de fosfina) cercana al 100%. MoO_3/TiO_2 no permitió la oxo-transferencia sugiriendo la importancia del ligando bipiridinico como una conexión electrónica entre la unidad MoO_2L y el TiO_2. Adicionalmente, se observó que cuando se incrementa el flujo fotónico, el rendimiento cuántico y la concentración inicial de la PPh_3, aumenta la velocidad de reacción de la TAO para el sistema MoO_2L/TiO_2.

1. Introduction

The direct use of molecular oxygen as an oxidant for the selective oxidation of organic compounds requires activation of O_2 by transforming the triplet spin state in order to allow the reaction with organic substances [1, 2]. The traditional activation of oxygen is done by thermal action at least 400K, with probability of explosion [3]. An alternative activation procedure is using a pathway of lower activation energy, through the formation of a metal-dioxygen complex [*M (paramagnetic)-O_2*] (doublet state): $[M^n{+}^3O_2\,(\cdot O-O\cdot)\,M^{n+1}\,(O_2)$. (doublet state) which can selectively react with organic molecules (R-H), following a similar mechanism to autoxidation. Coordination of O_2 to a complex with metal oxo (M=O) unit [4–6] permits the transfer of oxygen atom to organic molecules under mild reaction conditions but requires an oxygen donor agent to regenerate the metaloxo center [7]. The (Mo^{VI} = O_2L) (L is bipyridine, thiocyanate) has

* Corresponding author: Julián E. Sánchez Velandia
E-mail: julian.sanchezv@udea.edu.co
ISSN 0120-6230
e-ISSN 2422-2844

been used for Oxygen Atom transfer (OAT) [8, 9]. The OAT process begins by the nucleophilic attack of the compound (X) on an empty Mo=O π^* orbital, forming XO and Mo^{IV} species [10]. The initial reaction depends on the oxo-donor center nucleophilicity or electrophilicity. Generally, the re-oxidation of Mo^{IV} is based on an oxygen donor such as DMSO, which is used as a solvent in the reaction, but it can generate unwanted by products [11].

The anchoring of dioxomolybdenum complexes on TiO_2: ($Mo^{VI}O_2L/TiO_2$) favors the OAT to the organic substance under UV radiation and allows to use molecular oxygen as oxidant agent [12]. Our experience showed that the re-oxidation of the reduced metal center ($Mo^{IV}O)L/TiO_2$) with O_2 and without light is able to continue the catalytic cycle [13].

The OAT kinetics has been studied with several dioxo-molybdenum complexes in solution [14], using triphenylphosphine (PPh_3) as the oxygen acceptor. However, there are no studies on the kinetics of a heterogeneous system like $Mo^{VI}O_2L/TiO_2$ that works with light and molecular oxygen.

In this work, the effect of kinetic parameters (initial concentration of PPh_3, photonic flux, and the quantum yield) of the photoinduced OAT were studied to PPh_3 with 4,4'-dicarboxylate-2,2'-bipyridine-dioxodichloromolybdene, molybdic acid and molybdenum oxide, anchored to TiO_2 with molecular oxygen as the oxidant agent.

2. Experimental methodology

2.1 Catalyst synthesis

4,4'-dicarboxylate-2,2'-bipyridine-dioxo-dichloro molybdenum anchored to TiO_2 ($BipyMoO_2/TiO_2$)

0.120 g of 4,4'-dicarboxi-2,2'-bipyridine acid (Aldrich, 70% wt) was dispersed on 40 mL of benzene and 0.102 g of 1,3 *Bis*-trimethyl silil urea (Aldrich, 95% wt) and was stirred for 4h at room temperature. After, the solid was filtered and the excess of solvent was evaporated, a white solid called Bipy-Sil (A) was obtained. 0.5 mmol of A was dissolved on 40 mL of benzene and in a solution of 0.5 mmol of MoO_2Cl_2 in 30 mL of the same solvent, stirring for 4h at room temperature until the formation of a solid (B). Finally, 0.294 g of B in 30 mL of benzene was added to 1 g of dehydrated TiO_2 (Degussa P-25) at constant stirring (400 rpm) for 12h. The resultant solid ($BipyMoO_2/TiO_2$, Figure 1a) was filtered and washed with benzene. As benzene is a very toxic solvent, other green solvents could be used for this application (Toluene, heptane or DMF that are less toxic and have been used for silylation of secondary amines) [15].

Molybdic acid anchored to TiO_2 (H_2MoO_4/TiO_2)

0.294 g of molybdic acid (Aldrich) in 30 mL of benzene was added to 1.0 g of dehydrated TiO_2 (Degussa P-25) at constant stirring (400 rpm) for 12 h. Finally, the solid was washed with benzene (Figure 1b). The same consideration for increasing the sustainability of the synthesis could be taken into account, changing the solvent for others such as DMF [15].

Molybdenum trioxide anchored to TiO_2 (MoO_3/TiO_2)

The catalyst was synthesized according to [16]. For this, 5.52 mL of ammonium heptamolybdate tetrahydrate (Aldrich 97% wt) was added dropwise over 2.1077 g of dehydrated TiO_2 at constant stirring (400 rpm) for 1 h. Finally, the solid was dried at 383 K for 16 h and calcined in air at 773 K for 6h (Figure 1c)

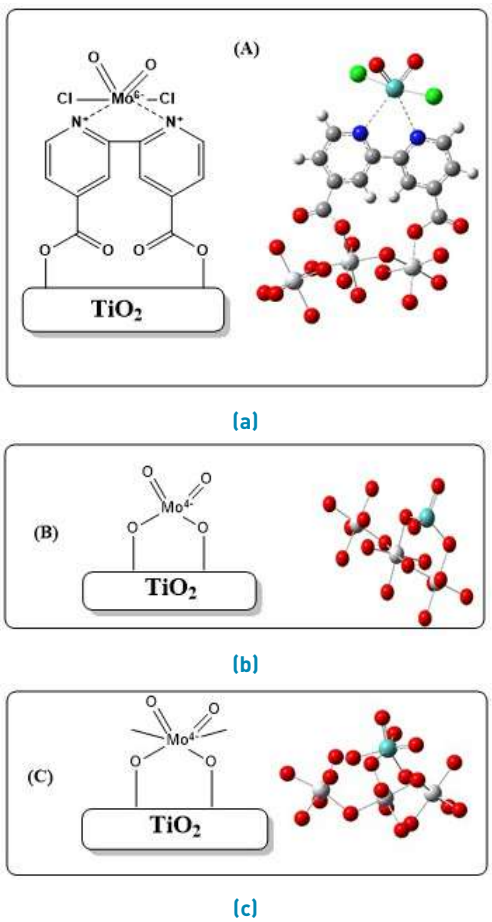

Figure 1 Scheme of the synthesized catalyst. In each figure, the molecular structure is shown: A) $BipyMoO_2/TiO_2$ B) $AcMo/TiO_2$ and C) MoO_3/TiO_2

2.2 Characterization of catalysts

The specific area BET (Brunauer-Emmett-Teller) and the pore volume were determined using the adsorption-desorption isotherms of N_2 in a Micromeritics 3 flex equipment at 77 K. Samples were degasified at 523 K for 30 min previously to the analysis. FTIR spectra were taken in an infrared spectrometer Bruker tensor 27 using a NaCl cell at 32 scans. To estimate the amount of anchored complex, TGA was performed using a thermogravimetric analyzer model 5,500, with a heating rate of 10°C/min and a nitrogen atmosphere from 298 K to 1,073 K. UV-Vis diffuse reflectance measurements were acquired in a Shimadzu UV-Vis RD spectrometer model 2,401. For the Raman spectra, an Evolution Horiba confocal microscope was used, with 10x objective, 2s integration time and 10 accumulations. Atomic absorption was performed to determine the amount of metal in all catalysts. For this, 50 mg of each material was dissolved on a mix of HF/HCl/HNO_3 and measured in an atomic absorption equipment Philips PU9100X model. The powder XRD was not included because of the quantity of each Mo catalyst is low and only detected phases anatase and rutile of TiO_2.

2.3 Catalytic activity

The photocatalytic reactions were carried out in a 15 mL microreactor Batch type (Aceglass), with a pen-ray lamp (λ_{max} = 360 nm), 60 mg of catalyst and 10 mL of 0.01 M of PPh_3 (acetonitrile as solvent) was used at 293 K. Initially, the reaction was left 1 h with an atmosphere of nitrogen (purge) and in the darkness to eliminate possible radical species $(O_2{}^{\cdot -}, {}^{\cdot}OH, HO_2{}^{\cdot})$. Afterward, it was changed under an oxygen atmosphere for 30 min before the light turns. Finally, the catalytic reaction was put in a way (60 mg of catalyst, 10 mL of 0.01 M of PPh_3 with acetonitrile as solvent at 293 K). The Selection of the amount of catalyst was based on previous results [17].

The formation of triphenylphosphine oxide ($OPPh_3$) was determined with UV-Vis spectroscopy, measuring the P=O band ($n \rightarrow \pi^*$) at 265 nm [18] and the PPh_3 band at 258 nm [19]. The kinetic study was performed varying the initial concentration of PPh_3, photonic flux, and quantum yield.

The determination of photonic flux was carried out using chemical actinometry [20, 21] using the Reinecke salt ($K[Cr(NH_3)_2(NCS)_4]$) and measuring the absorbance from 350 nm to 750 nm. The measures were performed with two Pen-ray lamps with a λ_{max}=360 (with two different voltages: 280 V and 375 V). The NCS ion generation rate was determined from the complexation with $Fe(NO_3)_3{}^{\cdot}9H_2O$ in $HClO_4$ at 432 nm. The photonic fluxes determined were 321.54 μEinsteinL^{-1}min^{-1} y 8360.13 μEinstenL^{-1}min^{-1}, respectively.

The quantum yield was estimated using the equation reported previously [22, 23] for heterogeneous photocatalytic systems (Equation 1):

$$\phi = \frac{\left(\frac{V_T}{V_r}\right)\left(\frac{dC_{tph}}{dt}\right)_{t=0}}{LVRPA} \quad (1)$$

Where V_T represents the total volume of the reactor, V_r the volume used for the reaction, $\left(\frac{dC_{tph}}{dt}\right)_{t=0}$ is the variation of the concentration at the initial time of the triphenyl phosphine and $LVRPA$ is the local volumetric rate of photon absorption.

LVRPA can be estimated using the equation (Equation 2) [24, 25].

$$LVRPA = F_e\left(1 - e^{-\mu\varphi}\right) \quad (2)$$

Where F_e represents the radiation in the reaction system, $\mu = C_{cat}K_\lambda$ (C_{cat} is the concentration of catalyst and K_λ is the specific absorption coefficient) and φ is the reactor diameter.

3. Results and analysis

3.1 Characterization of the materials

Figure 2 shows the IR spectra for all molybdenum materials. The presence of Mo-pyridine anchored on titanium oxide (Figure 2a), was determined with the bands at 1,395 cm^{-1} and 1,797 cm^{-1} related to the C-O and C=O vibrations [26]. The presence of the bipyridine ligand was confirmed with the bands at 1,591 cm^{-1} and 1,797 cm^{-1} associated with the C=C and C=N vibrations [27, 28] and the signals at 940 cm^{-1} and 915 cm^{-1} corresponding to the symmetric and asymmetric vibrations of the MoO_2 group, respectively [29]. The molybdic acid supported on titania (Figure 2b) shows bands at 500 cm^{-1} and 600 cm^{-1} due to TiO_2 while that OH group present bands at 1,620 cm^{-1} and 3,100 cm^{-1} (related to geminal and terminal groups of the titanium oxide) [30]. The dioxo-Mo compound show bands at 894 (asymmetric) and 945 cm^{-1} (symmetric) and at 721 cm^{-1} associated with the Mo-O stretching vibration [31, 32]. On the other hand, The MoO_3/TiO_2 (Figure 2c) system presents bands at 867 and 831 cm^{-1} [32] related to the symmetric and asymmetric vibrations of the MoO_2 group, respectively [30].

Figure 3 show the UV-Vis spectrum of the Mo supported materials which presents an asymmetric band at around 360 nm associated with the charge transference ligand-to-metal $(O^{2+} \rightarrow Mo^{6+})$ [10, 33, 34]. The Mo anchored on TiO_2 bandgap is evaluated with the UV-Vis spectra, according to Equation 3 [35, 36].

$$(ahv)^{\frac{1}{2}} = A_1(hv - E_g) \quad (3)$$

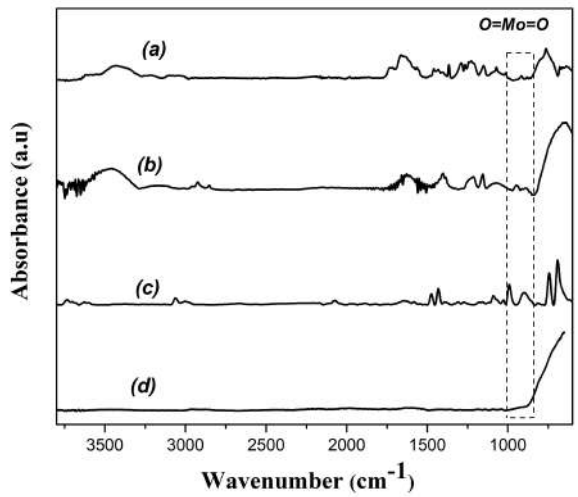

Figure 2 IR spectra of Mo supported heterogeneous catalysts: a) $BipyMoO_2/TiO_2$ b) $AcMo/TiO_2$ c) MoO_3/TiO_2 d) TiO_2

Where $h\upsilon$ is the photon energy, A_l is the independent parameter of the photon energy for the complex transitions, and E_g is the band-gap energy. The calculated values of the band-gap of $BipyMoO_2/TiO_2$ give a value of 3.2 eV, with the same values for the other Mo systems, suggesting that the TiO_2 band-gap was not affected after anchoring the Mo compounds.

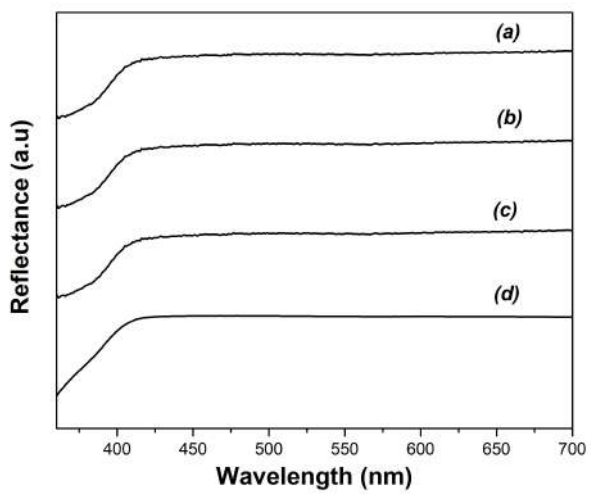

Figure 3 UV-Vis spectra of Mo heterogeneous catalysts: a) $BipyMoO_2/TiO_2$ b) $AcMo/TiO_2$ c) MoO_3/TiO_2 d) TiO_2 catalysts

Figure 4 shows the Raman spectra of the $AcMo/TiO_2$ and MoO_3/TiO_2 catalysts. $AcMo/TiO_2$ (Figure 4a) presents bands at 958 cm^{-1} related with Mo=O vibration, 950 cm^{-1} associated with the symmetric vibration of Mo-O-Mo group, symmetric bending at 689 cm^{-1} and the deformation of Mo-O-Mo at 249 cm^{-1} [37, 38]. Molybdic acid supported on TiO_2 presents the anatase phase of TiO_2 signals due to vibrational modes E_g, B_{1g} and A_{1g} at 136, 322, 397, 517, and 639 cm^{-1} [39, 40]. Also, a small signal is observed at 962 cm^{-1} that corresponds to the Mo=O bond stretch. In the case of the MoO_3/TiO_2 catalyst (Figure 4b), a characteristic band at 114 cm^{-1} related to the vibrational mode of Ti-O (E_g) is present. Bands at 125 cm^{-1}(B_{3g}), 157 cm^{-1} (A_g, B_{1g}), 663 cm^{-1} (B_{2g}, B_{3g}), 195 cm^{-1} (B_{2g}), 217 cm^{-1} (A_g), 244 cm^{-1} (B_{3g}), 289 cm^{-1} (B_{2g}, B_{3g}), 335 cm^{-1} (B_{1g}, A_g), 336 cm^{-1} (A_g), 469, 993 cm^{-1} and 816 cm^{-1}(A_g, B_{1g}) associated with the symmetric vibrations Mo=O, Mo-O-Mo (symmetric and non-symmetric vibration), Mo=O (terminal vibration) and the symmetric and non-symmetric vibrations of the MoO_2 were also detected. *In-situ* Raman and IR spectroscopic studies suggest that dehydrated metal oxide species presents a M = O terminal bond (where M is V, Mo, or Cr) [41].

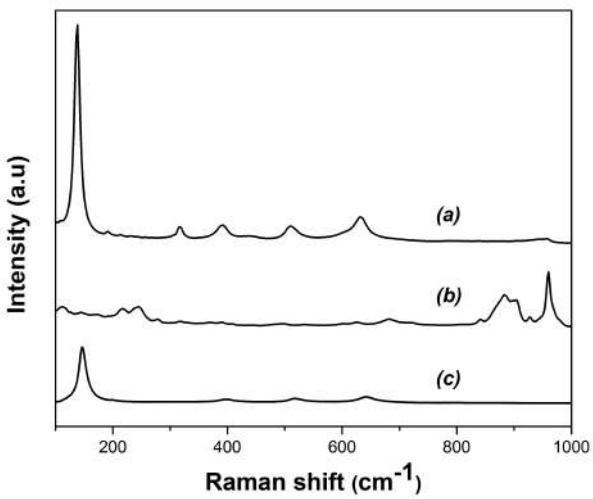

Figure 4 Raman spectra of Mo heterogeneous catalysts: a) $AcMo/TiO_2$ b) MoO_3/TiO_2 c) TiO_2 catalysts

Table 1 presents the textural properties of the synthesized materials. The system (MoO_3/TiO_2) has the highest amount of Mo per gram of catalyst and the smallest surface area, with a considerably larger pore diameter in comparison with the bipyridine system. In the case of $AcMo/TiO_2$, which has a lower amount of Mo, it has an intermediary surface area. In all cases, it is observed that the incorporation of Mo on the support considerably decreases the BET surface area. In the case of the $AcMo/TiO_2$ and MoO_3/TiO_2 catalysts, the BET area is almost 50% as compared to TiO_2. The decreasing of the surface area compared to titanium oxide (Degussa P-25) can be attributed to increasing of the dispersion of Mo species. In contrast with other Mo supported catalysts, it has been showed that, increasing the MoC (Molibdenun carbide) onto TiO_2 supported (12.0% wt) presents a similar

Table 1 Textural properties of the Mo-heterogeneous catalysts

Catalyst	Surface area (m^2/g)	Pore volume (cm^3/g)	Pore diameter (Å)	mmol Mo/g catalyst*
TiO_2 - degussa P25	49	- - - - -	- - - - -	0.00
$BipyMoO_2/TiO_2$	43	0.0054	289	0.15**
$AcMo/TiO_2$	26	0.0049	337	0.13
MoO_3/TiO_2	23	0.0029	329	0.52

* Values determined using atomic absorption.

** TGA determined this value.

Table 2 Catalytic activity of the different Mo supported catalysts

Catalyst	Conversion (%)	Selectivity to $OPPh_3$	TON	TOF (h^{-1})
$BipyMoO_2/TiO_2$	96	$>$ 95	5.92	9.66
$AcMo/TiO_2$	95	4*	3.95	12.17
MoO3/TiO_2	93	15*	1.03	1.53

*Reaction conditions: 0.01 M of PPh_3 in acetonitrile (10 mL), 60 mg of catalyst, 450 rpm at room temperature. Conversion and selectivity were calculated at 240 min. TON was calculated as mmol of PPh_3 per mmol of Mo (t=30 min). TOF was taken as the first derivate of TON with respect to time at saturation regime and instantaneous conditions (TOF=(dTON/dt) $_{t=1\ min}$). *Other by products were obtained but not identified.

surface area than TiO_2 degussa P25 [42]. $AcMo/TiO_2$ and MoO_3/TiO_2 presents similar surface area to Mo (0.02% - 0.1%) doped TiO_2 [43].

3.2 Effect of the photocatalytic parameters: Estimation of the oxo-transfer kinetics

The kinetics of the photo-oxidation of triphenylphosphine was performed using $BipyMoO_2/TiO_2$, MoO_3/TiO_2 and $AcMO/TiO_2$ catalysts, taking into account the effect of the initial concentration, photonic flux and the quantum yield. Blank reactions were carried out: without catalyst (oxygen atmosphere) and with catalyst and without light. It is observed that the oxidation of triphenylphosphine is not carried out in presence of oxygen and without light. TiO_2 support without light did not show activity towards oxygen transfer to phosphine. In this way, Table **??** shows the catalytic oxo-transfer activity of different Mo supported catalysts. It can be seen that the highest conversion and selectivity to $OPPh_3$ was obtained with $BipyMoO_2/TiO_2$. $BipyMoO_2/TiO_2$ presents the highest TON (at 30 min), suggesting that the bypyridine ligand favor the oxo-transfer to PPh_3. Also, the electronic transference from TiO_2 favor oxygen donation by decreasing the Mo=O bond order [12].

Effect of the photonic flux

Figure 5 shows the effect of the radiation intensity in the concentration of PPh_3 as a function of time. It can be seen that when increasing photonic flux, the phosphine transforms rapidly. Similar behavior is observed with the three Mo-catalytic systems. The photocatalytic support properties remain the same, which could be associated to the location of Mo species in the material.

The kinetic was evaluated, calculating the specific rate constant, using the Langmuir-Hinshelwood-Hougen-Watson (LHHW) model (Equation 4), which gives the best fitting in comparison with other pseudo-homogeneous (o polynomial) kinetic models. It was considered that the limiting step corresponds to the surface reaction and that the heat of adsorption is constant in the surface (ideal model) [44, 45].

$$r_a = -\frac{\mathrm{d}\left[\mathrm{PPh_3}\right]}{\mathrm{dt}} = \left(\frac{\mathrm{kK}\left[\mathrm{PPh_3}\right]}{1+\mathrm{K}\left[\mathrm{PPh_3}\right]}\right) \qquad (4)$$

Where $[PPh_3]$ means the concentration of the substrate, k is the kinetic constant (associated with the product of the quantum yield and the volumetric rate of absorption of photons (F_{abs})) y K is the adsorption constant [44, 45]. The kinetic was considered as first-order because oxygen is in excess in comparison with the other reactants: solvent and catalyst present in the reaction.

Table 3 indicates the specific rate constants estimated for each catalyst as a function of photonic flux. It can be observed that the catalytic system $BipyMoO_2/TiO_2$ presented the highest rate constant for both photonic

Table 3 The specific reaction rate constant of the Mo heterogeneous catalysts

Catalyst	Lamp 1: Photonic flux of 321.54 EinstenL^{-1}min^{-1}	Lamp 2: Photonic flux of 8,360.13 μEinstenL^{-1}min^{-1}
	$k_{specific} \pm \triangle k(min^{-1})$	$k_{specific} \pm \triangle k(min^{-1})$
BipyMoO$_2$/TiO$_2$	0.014±0.005	0.040±0.008
AcMo/TiO$_2$	0.011±0.004	0.017±0.007
MoO$_3$/TiO$_2$	0.012±0.003	0.013±0.008

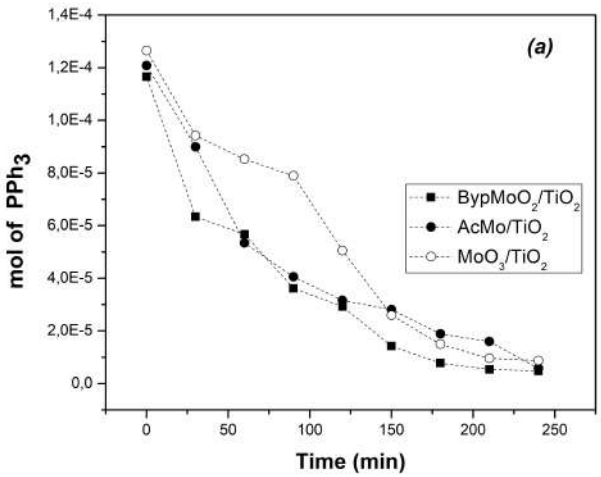

(a)

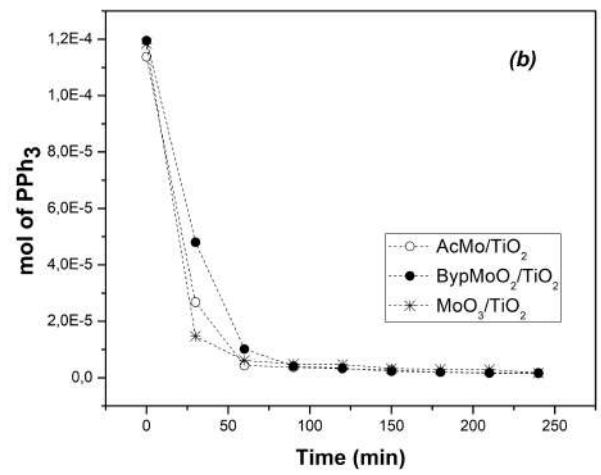

(b)

Figure 5 Photocatalytic transformation of PPh_3 as a function of the time with the lamp of a photonic flux of (a) 321.54 μEinsteinL^{-1}min^{-1} and b) 8360.13 μEinsteinL^{-1}min^{-1}. **Reaction conditions:** Room temperature, acetonitrile as the solvent (10 mL), constant stirring (450 rpm), and 60 mg of catalyst

fluxes. It could be associated with the conductive nature of the bipyridine ligand, which favors the electronic conduction between the dioxo-Mo and the semiconductor surface. It is correlated with the highest generation of the $OPPh_3$.

Given the observed correlation between the increase in photonic flux (8,360.13 μEinstenL^{-1}min^{-1}), and the significant increase of the velocity constant, it can be seen that with this lamp, the kinetic constant is almost four times higher than the other one. In the case of the AcMo/TiO_2 and MoO_3/TiO_2 catalysts, there is no noticeable change when increasing the photon flux, which may suggest that the oxidation mechanism is different.

When the BipyMoO$_2$/TiO_2 catalyst is used, the formation of $OPPh_3$ (triphenylphosphine oxide) as a function of time corresponds to 1:1 molar ratio between PPh_3 and $OPPh_3$ (Figure 6), which is associated to the transference of the oxygen atom from dioxo-Mo to phosphine, according to the OAT mechanism. While for the other two catalysts (Figure 6b and 6c), this molar ratio is different, generating other oxidation products via a radical pathway (Figure 7) [46]. This is because between the Mo unit and the support does not exist a good electronic connection as occurs with BipyMoO$_2$/TiO_2. Besides, for the AcMo/TiO_2 system (Figure 6b), and MoO_3/TiO_2 (Figure 6c), the stoichiometric ratio is not 1:1 evidencing that the mechanism is a radical pathway instead of an electronic transfer.

Effect of the initial concentration

The initial concentration of the reactant affects the oxidation rate. To evaluate the effect of concentration, the following solutions of PPh_3 0.01, 0.005 and 0.001 M were taken, and the catalytic activity was observed at the same reaction time, using a photonic flow of 321.54 μEinstenL^{-1}min^{-1}.

Figure 8 shows the effect of the concentration for each catalyst. The increase in concentration generates an increase in the specific reaction rate constant in each case (Table 4).

It was observed that the BipyMoO$_2$/TiO_2 catalyst showed that the rate constant is a function of the concentration. The activity of AcMo/TiO_2 changes slightly with the initial

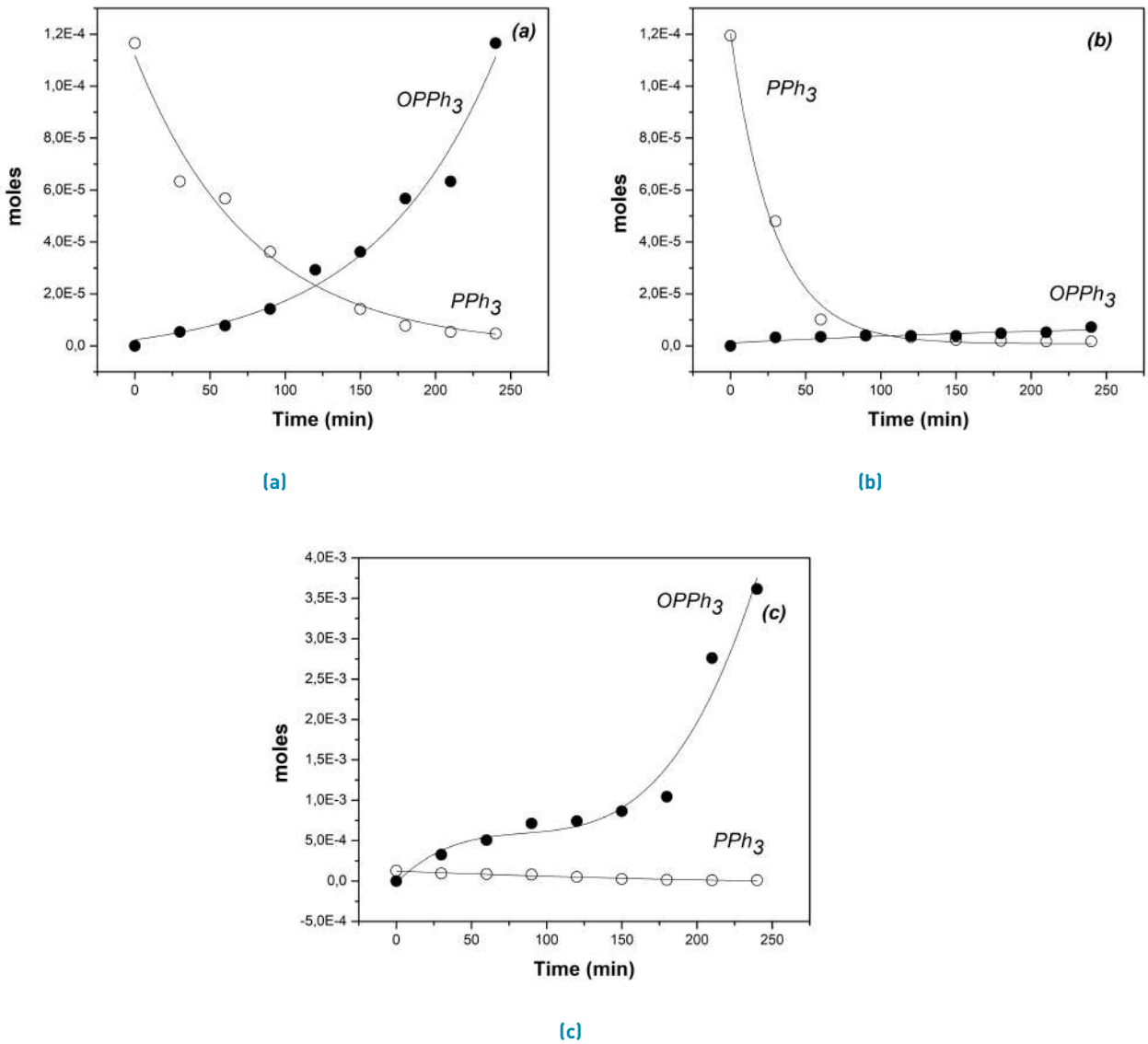

Figure 6 Generation of $OPPh_3$ as a function of the time: (a) $BipyMoO_2/TiO_2$ (b) $AcMo/TiO_2$ and (c) MoO_3/TiO_2. **Reaction conditions:** Room temperature, acetonitrile as the solvent (10 mL), constant stirring (450 rpm), and 60 mg of catalyst

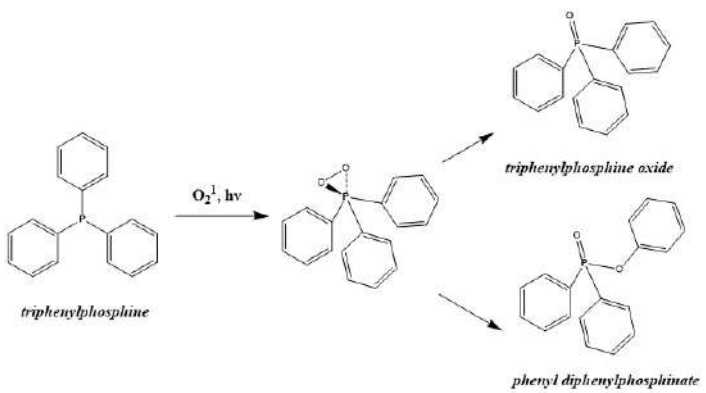

Figure 7 Formation of different products of the oxidation of PPh3 on time towards a radical pathway. Modified from reference [46]

Table 4 The specific rate constant of reaction as a function of the initial concentration of PPh_3

Catalyst	0.01 M	0.005 M	0.001 M
	k specific $\pm$ $\triangle$k(min^{-1})	$k_{specific}$ $\pm$ $\triangle$k(min^{-1})	$k_{specific}$ $\pm$ $\triangle$k(min^{-1})
$BipyMoO_2/TiO_2$	0.014$\pm$0.005	0.011$\pm$0.005	0.003$\pm$0.006
AcMo/TiO^2	0.011$\pm$0.004	0.008$\pm$0.007	0.005$\pm$0.007
MoO_3/TiO_2	0.013$\pm$0.003	0.011$\pm$0.005	0.001$\pm$0.006

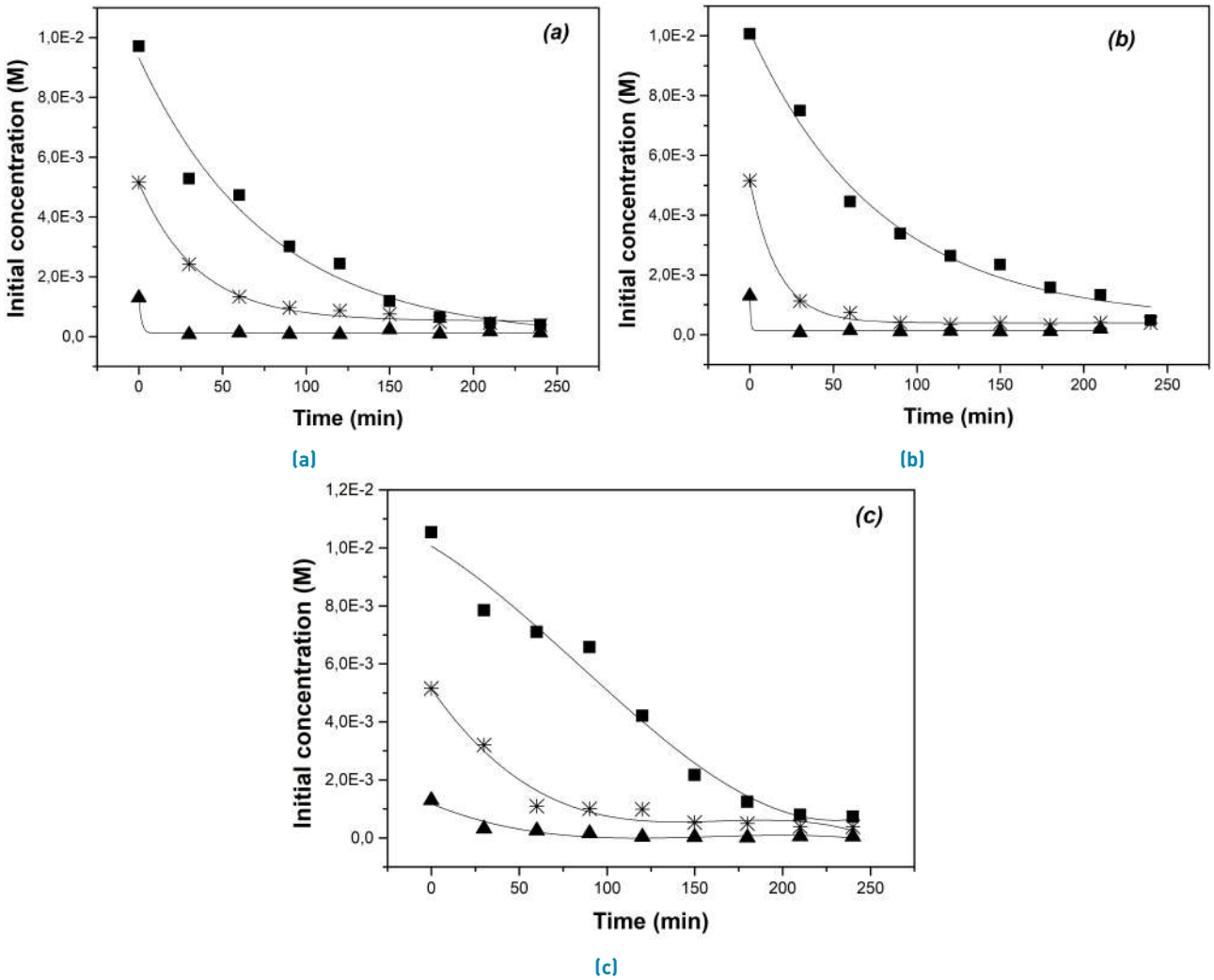

Figure 8 Effect of the initial concentration for Mo-heterogeneous catalysts: (a) $BipyMoO_2/TiO_2$ (b) $AcMo/TiO_2$ and (c) MoO_3/TiO_2. **Reaction conditions:** Room temperature, acetonitrile as the solvent (10 mL), constant stirring (450 rpm), and 60 mg of catalyst. (Symbols indicate the tendency of each initial concentration; squares=0.01 M, asterics=0.006 M and triangles=0.002 M)

concentration, and its value does not increase significantly as a function of concentration. At the same time, in the other two cases, the specific constant varies significantly. When the concentration is 0.01 M, the constant presents a maximum for $BipyMoO_2/TiO_2$. In contrast, for the concentration of 0.005 M, the kinetic behavior was higher for MoO_3/TiO_2, perhaps associated with its higher concentration of Mo.

Estimation of the quantum yield and their effect

Estimation of the quantum yield was calculated using the Equations 1 and 2. Figure 9 shows the variation of the reaction kinetic constant as a function of the quantum yield for each Mo catalyst. Increasing the quantum yield, the initial reaction rate increases for all catalysts; nevertheless, the behavior is different for the MoO_3/TiO_2 material, where the increase of reaction rate is slowest; this fact could be associated with the

Table 5 Comparison of Quantum Yields for different heterogeneous photocatalysts

Catalyst	Substract	Reaction conditions	Quantum Yield (einstein s^{-1})	Reference
TiO_2 (Degussa P-25)	Phenol 2,6-dimethylphenol	Photodegradation, 200 μm of substract, 2 gL^{-1} of catalys, pH=3	0.11±0.01 0.33±0.02	[47]
Colloidal TiO_2	Formaldehyde	100 mgL^{-1} of catalyst, pH=2, 100 mM of sustrate	0.02	[48]
TiO_2 (Degussa P-25)	Phenol	Photodegradation, 50 mg/L of substract, 1 gL^{-1}	0.13 (0.02*)	[49]
$BipyMoO_2/TiO_2$ $AcMo/TiO_2$ MoO_3/TiO_2	Triphenylphosphine	0.01 M of substract, 10 mL of solvent, 6 g L^{-1} of catalyst	0.67 0.85 0.33	This work

*If not considering the absorption coefficient of the incident light.

amount of Mo. As for both $BipyMoO_2/TiO_2$ and $AcMo/TiO_2$ catalysts, the same amount of Mo was added, a similar quantum yield behavior was achieved. Other reason for this fact could be associated with the variation of the reaction rate, the photonic flux and the absorption coefficient, which are associated mainly with the TiO_2 support. It was assumed that only TiO_2 contributes to the photocatalytic properties of the material, and besides, that other properties are considered constant (scattering and absorption coefficients). The quantum yields are lower than 25 Einstein min^{-1}; the reaction rate appears to be the same for the three catalysts and by increasing the quantum yield, the reaction rate increases exponentially for all materials.

As no detailed kinetics have been reported, the current study shows references values of quantum yield (at different conditions) of Mo catalysts supported on TiO_2, characteristic of photocatalysts used in different applications. As can be seen in Table 5, all heterogeneous catalysts present a quantum yield in a range between 0 and 0.9 Einstein s^{-1}, being our system $AcMo/TiO_2$, the higher as compared with the other materials. It is essential to highlight that in all cases, only TiO_2 was used. The lowest value was achieved for the colloidal TiO_2 used for the degradation of formaldehyde (0.019). Similar yields were obtained towards the degradation of phenol with TiO_2 (Degussa P-25) (0.11-0.1275). Also, the quantum yield obtained for the MoO_3/TiO_2 catalyst showed the same value that TiO_2 (Degussa P-25) used for the degradation of 2.6-dimethylphenol.

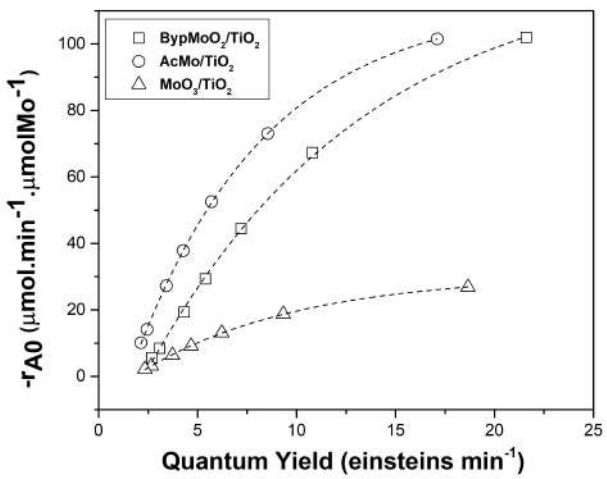

Figure 9 Effect of the quantum yield for Mo heterogeneous catalysts. **Reaction conditions:** room temperature, acetonitrile as the solvent (10 mL), constant stirring (450 rpm), and 60 mg of catalyst

4. Conclusions

The kinetics of the oxygen atom transfer reaction to triphenylphosphine with several Mo heterogeneous catalysts anchored to TiO_2 stimulated with the light was studied. The rate constant increases as the concentration of the triphenylphosphine as does the photonic flux and the quantum yield increases.

Molybdic acid, as molybdenum oxide anchored on TiO_2, does not allow oxygen atom transfer reaction, suggesting

the importance of the bipyridine ligand as an electronic connector between the Mo complex and TiO_2 that favor the transfer of oxygen.

This work corresponds to the first report of the kinetic effects of a reaction of heterogeneous photo-oxidation with dioxo-Mo compounds anchored to TiO_2.

5. Declaration of competing interest

None declared under financial, professional and personal competing interest.

6. Acknowledgments

The authors acknowledge the DIEF of the sciences faculty of the Universidad Industrial de Santander (project 1898) for their financial support and Parque Tecnológico de Guatiguará (PTG) for the physicochemical characterization.

References

[1] Z. Guo and *et al.*, "Recent advances in heterogeneous selectiveoxidation catalysis for sustainable chemistry," *Chemical Society Reviews*, vol. 43, pp. 3480–3524, 2014.

[2] R. Neumann and A. Khenkin, "Molecular oxygen and oxidation catalysis by phosphovanadomolybdates," *Chemical Communications*, vol. 24, pp. 2529–2538, Mar. 2006.

[3] S. Gosh and *et al.*, "Selective oxidation of propylene to propylene oxide over silver-supported tungsten oxide nanostructure with molecular oxygen," *ACS Catalysis*, vol. 4, no. 7, June 3 2014. [Online]. Available: https://doi.org/10.1021/cs5004454

[4] N. J. Castellanos, "Síntesis, caracterización y evaluación de la actividad foto catalítica de los complejos 1,10-fenantrolina-dibromo-dioxo-molibdeno(VI) y 1,10-fenantrolina-dicloro-dioxo-molibdeno (VI)," Undergraduate, Universidad Industrial de Santander, Bucaramanga, Colombia, 2005.

[5] N. J. Castellanos, "Estudio del efecto de ligandos N-heterocíclicos insaturados en la oxo-transferencia foto-inducida con complejos del tipo MoO_2Cl_2Ln/TiO_2," Ph.D. Dissertation, Universidad Industrial de Santander, Bucaramanga, Colombia, 2011.

[6] H. Arzoumanian, N. J. Castellanos, F. O. Martínez, E. O. Páez, and F. Ziarelli, "Silicon-assisted direct covalent grafting on metal oxide surfaces: Synthesis and characterization of carboxylate N,N'-Ligands on TiO_2," *European Journal of Inorganic Chemistry*, vol. 2010, no. 11, March 31 2010. [Online]. Available: https://doi.org/10.1002/ejic.200901092

[7] H. Arzoumanian, "Molybdenum-oxo and peroxo complexes in oxygen atom transfer processes with O_2 as the primary oxidant," *Current Inorganic Chemistry*, vol. 1, no. 2, 2011. [Online]. Available: https://doi.org/10.2174/1877944111101020140

[8] J. Kim, N. Ichikuni, T. Hara, and S. Shimazu, "Study on the selectivity of propane photo-oxidation reaction on SBA-15 supported Mo oxide catalyst," *Catalysis Today*, vol. 265, May 1 2016. [Online]. Available: https://doi.org/10.1016/j.cattod.2015.09.043

[9] R. A. Salamony, H. M. Gobara, and S. A. Younis, "Potential application of MoO_3 loaded SBA-15 photo-catalyst for removal of multiple organic pollutants from water environment," *Journal of water process Engineering*, vol. 18, August 2017. [Online]. Available: https://doi.org/10.1016/j.jwpe.2017.06.010

[10] P. Basu, B. W. Kail, and C. G. Young, "The influence of the oxygen atom acceptor on the reaction coordinate and mechanism of oxygen atom transfer from the dioxo-Mo(VI) complex, $Tp^{ipr}MoO_2(OPh)$, to tertiary phosphines," *Inorganic Chemistry*, vol. 49, no. 11, 2010. [Online]. Available: https://doi.org/10.1021/ic902500h

[11] J. M. Tunney, J. McMaster, and C. D. Garner, "Molybdenum and tungsten enzymes," in *Comprehensive Coordination Chemistry II*, J. A. McCleverty and T. J. Meyer, Eds. New York, USA: Elsevier Ltd, 2003, pp. 459–477.

[12] H. Martínez and *et al.*, "Photo-epoxidation of cyclohexene, cyclooctene and 1-octene with molecular oxygen catalyzed by dichloro dioxo-(4,4'-dicarboxylato-2,2'-bipyridine) molybdenum$^{(VI)}$ grafted on mesoporous TiO_2," *Journal of Molecular Catalysis A: Chemical*, vol. 423, November 2016. [Online]. Available: https://doi.org/10.1016/j.molcata.2016.07.006

[13] H. Martínez, . A. Amaya, E. A. Páez, and F. Martínez, "Highly efficient epoxidation of α-pinene with O_2 photocatalyzed by dioxoMo(VI) complex anchored on TiO_2 nanotubes," *Microporous and Mesoporous Materials*, vol. 265, February 2018. [Online]. Available: https://doi.org/10.1016/j.micromeso.2018.02.005

[14] M. S. Reynolds, J. M. Berg, and R. H. Holm, "Kinetics of oxygen atom transfer reactions involving oxomolybdenum complexes. general treatment for reactions with intermediate oxo-bridged molybdenum(V) dimer formation," *Inorganic Chemistry*, vol. 23, no. 20, September 1 1984. [Online]. Available: https://doi.org/10.1021/ic00188a007

[15] (1995) Silylating agents: Derivatization reagents, protecting-group reagents, organosilicon compounds, analytical applications, synthetic applications. Fluka Chemika. Accessed Mar. 25, 2020. [Online]. Available: https://bit.ly/2ykc4a2

[16] K. V. R. Chary, T. Bhaskar, G. Kishan, and V. Vijayakumar, "Characterization of MoO_3/TiO_2 (anatase) catalysts by ESR, ^{1}H MAS NMR, and oxygen chemisorption," *Journal of Physical Chemistry B*, vol. 102, no. 20, April 28 1998. [Online]. Available: https://doi.org/10.1021/jp980088r

[17] C. M. Flórez and M. Sánchez, "Fotoxidación catalítica del R(+)-limoneno por el dioxo-dibromo(4,4'-dicarboxilato-2,2'-bipiridina) de Mo$^{(VI)}$ soportado en dióxido de titanio (degussa P-25) (MoO_2/TiO_2 P-25)," Undergraduate, Universidad Industrial de Santander, Bucarmanga, Colombia, 2009.

[18] A. Palade and *et al.*, "Triphenylphosphine oxide detection in traces using MN(III)-5,10,15,20-tetratolyl-21h,23h porphyrin chloride," *Digest Journal of Nanomaterials and Biostructures*, vol. 10, no. 3, pp. 729–735, Jul. 2015.

[19] (2001) UV-Vis spectra of neutral bases and their protonated conjugated cationic acids in acetonitrile. Accessed Mar. 27, 2020. [Online]. Available: https://bit.ly/3abqel6

[20] E. E. Wegner and A. W. Adamson, "Photochemistry of complex ions. III. absolute quantum yields for the photolysis of some aqueous chromium(III) complexes. chemical actinometry in the long wavelength visible region," *Journal of the American Chemical Society*, vol. 88, no. 3, February 1 1966. [Online]. Available: https://doi.org/10.1021/ja00955a003

[21] J. F. Cornet, A. Marty, and J. B. Gros, "Revised technique for the determination of mean incident light fluxes on photobioreactors," *Biotechnology Progress*, vol. 13, no. 4, September 2008. [Online]. Available: https://doi.org/10.1021/bp970045c

[22] M. A. Mueses, F. Machuca, and J. Colina, "Determination of quantum yield in a heterogeneous photocatalytic system using a fitting-parameters model," *Journal of Advanced Oxidation Technologies*, vol. 11, no. 1, 2008. [Online]. Available: https://doi.org/10.1515/jaots-2008-0105

[23] F. Machuca, "Cálculo de parámetros cinéticos en reacciones foto-catalíticas usando un modelo efectivo de campo de radiación," *Ingeniería y Competitividad*, vol. 13, no. 1, 2011. [Online]. Available: https://doi.org/10.25100/iyc.v13i1.2681

[24] M. J. Muñoz, M. M. Ballari, A. Kubacka, O. M. Alfano,

and M. Fernández, "Braiding kinetics and spectroscopy in photo-catalysis: the spectro-kinetic approach," *Chemical Society Review*, vol. 48, no. 2, 2019. [Online]. Available: https://doi.org/10.1039/C8CS00108A

[25] O. M. Alfano, A. E. Cassano, J. Marugán, and R. V. Grieken, "Fundamentals of radiation transport in absorbing scattering media," in *Photocatalysis: Fundamentals and Perspectives*, J. Schneider, D. Bahnemann, J. Ye, G. L. Puma, and D. D. Dionysiou, Eds. cambridge, UK: Royal Society of Chemistry, 2016, pp. 140–156.

[26] (2018) Structure determination by spectroscopic methods. Oregon State University. Accessed Dec. 14, 2019. [Online]. Available: https://bit.ly/2VepUDU

[27] J. Grajeda, M. R. Kita, L. C. Gregor, P. S. White, and A. J. M. Miller, "Diverse cation-promoted reactivity of iridium carbonyl pincer-crown ether complexes," *Organometallics*, vol. 35, no. 3, November 19 2016. [Online]. Available: https://doi.org/10.1021/acs.organomet.5b00786

[28] J. Deerberg and *et al.*, "Stereoselective bulk synthesis of CCR2 antagonist BMS-741672: Assembly of an all-*cis* (*S,R,R*)-1,2,4-triaminocyclohexane (TACH) core via sequential heterogeneous asymmetric hydrogenations," *Organic Process Research & Development*, vol. 20, no. 11, October 13 2016. [Online]. Available: https://doi.org/10.1021/acs.oprd.6b00282

[29] C. Li, Q. Xin, K. L. Wang, and X. Guo, "FT-IR emission spectroscopy studies of molybdenum oxide and supported molybdena on alumina, silica, zirconia, and titania," *Applied spectroscopy*, vol. 45, no. 5, June 1 1991. [Online]. Available: https://doi.org/10.1366/0003702914336651

[30] S. Bagheri, K. Shameli, and S. B. Abd, "Synthesis and characterization of anatase titanium dioxide nanoparticles using egg white solution via sol-gel method," *Journal of Chemistry*, 2013. [Online]. Available: https://doi.org/10.1155/2013/848205

[31] P. Wongkrua, T. Thongtem, and S. Thongtem, "Synthesis of h- and α-MoO_3 by refluxing and calcination combination: Phase and morphology transformation, photocatalysis, and photosensitization," *Journal of Nanomaterials*, August 1 2013. [Online]. Available: https://doi.org/10.1155/2013/702679

[32] L. Seguina, M. Figlarza, R. Cavagnatb, and J. C. Lassègues, "Infrared and raman spectra of MoO_3 molybdenum trioxides and $MoO_3 \cdot xh_2o$ molybdenum trioxide hydrates," *Spectrochimica Acta Part A: Molecular and Biomolecular Spectroscopy*, vol. 51, no. 8, July 1995. [Online]. Available: https://doi.org/10.1016/0584-8539(94)00247-9

[33] S. Valencia, J. M. Marín, and G. Restrepo, "Study of the bandgap of synthesized titanium dioxide nanoparticules using the sol-gel method and a hydrothermal treatment," *The open Materials Science Journal*, vol. 4, June 19 2009. [Online]. Available: https://doi.org/10.2174/1874088X01004010009

[34] L. Galeano, J. A. Navio, G. M. Restrepo, and J. M. Marín, "Preparación de sistemas Óxido de titanio/Óxido de silicio (TiO_2/SiO_2) mediante el método solvotérmico para aplicaciones en fotocatálisis," *Información tecnológica*, vol. 24, no. 5, 2013. [Online]. Available: https://doi.org/10.4067/S0718-07642013000500010

[35] K. Nomiya, Y. Sugie, K. Amimoto, and M. Miwa, "Charge-transfer absorption spectra of some tungsten (VI) and molybdenum (VI) polyoxoanions," *Polyhedron*, vol. 6, no. 3, 1987. [Online]. Available: https://doi.org/10.1016/S0277-5387(00)81018-9

[36] J. Meyer and *et al.*, "Metal oxide induced charge transfer doping and band alignment of graphene electrodes for efficient organic light emitting diodes," *Scientific Reports*, vol. 4, p. 5380, Jun. 2014.

[37] M. Dieterle, G. Weinberg, and G. Mestl, "Raman spectroscopy of molybdenum oxides part I. structural characterization of oxygen defects in MoO_{3-x} by dr UV/VIS, raman spectroscopy and x-ray diffraction," *Physical Chemistry Chemical Physics*, vol. 4, no. 5, pp. 812–821, Jan. 2002.

[38] H. J. H. Knoezinger, "Raman spectra of molybdenum oxide supported on the surface of aluminas," *Journal of Physical Chemistry A*, vol. 82, no. 18, 2002. [Online]. Available: https://doi.org/10.1021/j100507a011

[39] E. J. Ekoi, A. Gowen, R. Dorrepaal, and D. P. Dowling, "Characterisation of titanium oxide layers using raman spectroscopy and optical profilometry: Influence of oxide properties," *Results in Physics*, vol. 12, March 2019. [Online]. Available: https://doi.org/10.1016/j.rinp.2019.01.054

[40] O.Frank and *et al.*, "Raman spectra of titanium dioxide (anatase, rutile) with identified oxygen isotopes (16, 17, 18)," *Physical Chemistry Chemical Physics*, vol. 14, no. 42, August 12 2012. [Online]. Available: https://doi.org/10.1039/C2CP42763J

[41] I. E. Wachs, "Raman and IR studies of surface metal oxide species on oxide supports: Supported metal oxide catalysts," *Catalysis today*, vol. 27, no. 3-4, February 1996. [Online]. Available: https://doi.org/10.1016/0920-5861(95)00203-0

[42] M. A. Hamdan, S. Loridant, M. Jahjah, C. Pinel, and N. Perret, "TiO'textsubscript2-supported molybdenum carbide: An active catalyst for the aqueous phase hydrogenation of succinic acid," *Applied Catalysis A: General*, vol. 571, December 2018. [Online]. Available: https://doi.org/10.1016/j.apcata.2018.11.009

[43] L. G. Devi and B. N. Murthy, "Characterization of mo doped TiO_2 and its enhanced photo catalytic activity under visible light," *Catalysis Letters*, vol. 125, no. 3, October 2008. [Online]. Available: https://doi.org/10.1007/s10562-008-9568-4

[44] J. M. Thomas and W. J. Thomas, *Principles and Practice of Heterogeneous Catalysis*, 2nd ed. Hoboken, NJ, USA: John Wiley & Sons, 2015.

[45] G. F. Froment, K. Bischoff, and J. de Wilde, *hemical Reactor Analysis and Design*, 3rd ed. Hoboken, NJ, USA: John Wiley & Sons, 2010.

[46] R. Gao and *et al.*, "Reaction of arylphosphines with singlet oxygen: intra- vs intermolecular oxidation," *Organic Letters*, vol. 3, no. 23, October 20 2001. [Online]. Available: https://doi.org/10.1021/ol010195v

[47] N. Serpone, "Relative photonic efficiencies and quantum yields in heterogeneous photocatalysis," *Journal of Photochemistry and Photobiology A: Chemistry*, vol. 104, no. 1-3, April 1997. [Online]. Available: https://doi.org/10.1016/S1010-6030(96)04538-8

[48] C. Wang, D. W. Bannemanm, and J. K. Dohrmann, "Determination of photonic efficiency and quantum yield of formaldehyde formation in the presence of various TiO_2 photocatalysts," *Water Science and Technology*, vol. 44, no. 5, February 2001. [Online]. Available: https://doi.org/10.2166/wst.2001.0306

[49] X. Yi and Y. Chun, "Calculation method of quantum efficiency to TIO_2 nanocrystal photocatalysis reaction," *Journal of Environmental Sciences*, vol. 14, no. 1, pp. 70–75, Feb. 2002.